

LA-UR-- 01-4412

Approved for public release;
distribution is unlimited.

Title: THE STABILITY OF THE PEROVSKITE COMPOUNDS
IN THE CE-GA-O AND PU-GA-O SYSTEMS

Author(s): Marius Stan, Tad J. Armstrong, Darryl P. Butt, Terry C. Wallace
Sr., YoungSoo Park, Carol L. Haertling, Thomas Hartmann, and
Robert J. Hanrahan Jr.

Submitted to: Journal of the American Ceramic Society



Los Alamos

NATIONAL LABORATORY

Los Alamos National Laboratory, an affirmative action/equal opportunity employer, is operated by the University of California for the U.S. Department of Energy under contract W-7405-ENG-36. By acceptance of this article, the publisher recognizes that the U.S. Government retains a nonexclusive, royalty-free license to publish or reproduce the published form of this contribution, or to allow others to do so, for U.S. Government purposes. Los Alamos National Laboratory requests that the publisher identify this article as work performed under the auspices of the U.S. Department of Energy. Los Alamos National Laboratory strongly supports academic freedom and a researcher's right to publish; as an institution, however, the Laboratory does not endorse the viewpoint of a publication or guarantee its technical correctness.

The Stability of the Perovskite Compounds in the Ce-Ga-O and Pu-Ga-O Systems

Marius Stan ^{a,+,*}, Tad J. Armstrong ^b, Darryl P. Butt ^{c,*}, Terry C. Wallace, Sr. ^a,
YoungSoo Park ^{a,*}, Carol L. Haertling ^{a,*}, Thomas Hartmann ^a, and Robert J. Hanrahan Jr. ^a

^a Los Alamos National Laboratory, Los Alamos, NM 87545

^b Univ. of Texas, Austin, TX 78712

^c Univ. of Florida, Gainesville, FL 32611

ABSTRACT

The stability limits of the CeGaO₃ and PuGaO₃ compounds, with respect to the partial pressure of oxygen and temperature, have been predicted by theoretical calculations. Using the results of the calculations as guidance, mixtures of CeO₂ and Ga₂O₃ have been prepared and thermally treated at 1273, 1473 and 1673 K, in atmosphere of air, argon or Ar 6%H₂. In samples annealed under low oxygen partial pressures a CeGaO₃ perovskite type phase was identified. Based on Rietveld structure refinement, the orthorhombic space group (Pnma, 62) was confirmed.

+ Corresponding author: tel: 505-667-8726, fax: 505-667-8021, e-mail: mastan@lanl.gov

* Member, American Ceramic Society

1. INTRODUCTION

One of the keys to successful utilization of weapons grade Pu in mixed oxide fuel is to make it acceptable for nuclear plants. An important requirement is to minimize the concentration of trace elements not normally present in reactor fuel. Of these elements, the most significant is Ga, which in the weapons grade material is added to stabilize the fcc delta phase of Pu. In attempting to remove Ga from weapons grade Pu we wish to remove practically all of the Ga. Numerous experiments have shown that we can remove greater than 99% of the Ga with thermal treatments in a reducing atmosphere, by reducing Ga_2O_3 to the volatile compound Ga_2O . The solubility of Ga in PuO_2 is low, however, it is possible for a few ppm of Ga to go into solution. As the level of Ga in the PuO_2 approaches the solubility limit, this is thought to result in a solid-state diffusion limited transport regime [1].

Another possibility that would result in a limitation to the Ga evolution kinetics would be the formation of intermediate compounds in the Pu-Ga-O system, like a perovskite type phase. Such phases might exhibit slower reaction kinetics than Ga_2O_3 and thereby control the level of maximum Ga removal in any given thermal treatment. The perovskite phase may also affect the sintering mechanism in the pellets processed at low oxygen partial pressure, since the Ga appears to segregate to grain boundaries in these samples [2, 3].

The objective of the research discussed here is to estimate whether ternary phases are present in the Pu-Ga-O system using a combination of thermodynamic evaluations of available data, and experiments on the Ce-Ga-O system, where Ce is used as a substitute (i.e. surrogate) for

Pu. Understanding the Ce-Ga-O system might be the key to understand the Pu-Ga-O system and eventually the MOX fuel materials.

The crystal structures of CeO_2 , Ce_2O_3 and Ga_2O_3 are known, as well as the x-ray diffraction patterns [4]. Studies on rare earth gallates [5, 6] pointed out that their crystal structure is a tetragonal or an orthorhombic derivation of the cubic BaTiO_3 perovskite structure type. The actual structure of the mineral perovskite (CaTiO_3) is a small distortion of the ideal cubic $\text{Pm}\bar{3}\text{m}$ space group and at high temperatures the orthorhombic structure type is preferred. Rare earth gallates like CeGaO_3 and GdGaO_3 have been found to be isostructural to the equivalent CeFeO_3 , GdFeO_3 orthoferrites [7].

Marezio *et al.* [5] imply that the CeGaO_3 or PuGaO_3 compounds can be made only at high pressures while Geller *et al.* [6] reported fabricating $(\text{Ln})\text{GaO}_3$ type compounds at normal atmospheric pressure. They quenched equimolar proportions of the appropriate oxides, from high temperatures. Their experiments involved most of the lanthanides but CeGaO_3 was not the subject of any x-ray diffraction study by the authors. Interpolation of the values reported by Geller *et al.* for the lanthanide gallates allowed for the following estimation of lattice parameters of a possible CeGaO_3 perovskite structure: $a = b = 5.490 \text{ \AA}$, and $c = 7.749 \text{ \AA}$.

Synthesis of CeGaO_3 , by arc melting, has been recently reported by Shishido *et al.* [8]. In their work, the decomposition of CeGaO_3 into CeO_2 and Ga_2O_3 was described for temperatures above 1000 K. They argue that the structure is tetragonal (space group $\text{P4}/\text{mmm}$) and the lattice parameters are: $a = b = 3.873 \text{ \AA}$, and $c = 3.880 \text{ \AA}$.

This study was intended to provide the stability limits of the compound, the lattice parameters, and the x-ray diffraction pattern.

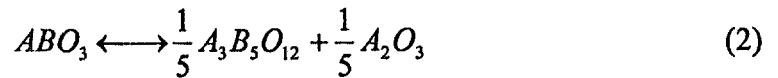
2. THERMODYNAMIC CALCULATIONS

The generic reaction leading to formation of compounds of perovskite type structure is:

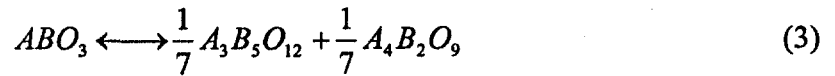


To choose a good surrogate for plutonium we have examined the situations where A = Ce or Pu, and B = Fe, Cr, Al or Ga. Fig.1 shows the Gibbs free energy of formation of the oxides that are involved in the process. One can note that Ce₂O₃ and Pu₂O₃ have similar free energies, the difference being smaller than 50 kJ/mol. The similar thermodynamic properties suggest using the cerium oxide as a surrogate for the plutonium oxide for this study.

The compounds with ABO₃ perovskite-type structure could also disproportionate [9] into a garnet-type compound (A₃B₅O₁₂) and a sesquioxide (A₂O₃):



A "two to one" phase (A₄B₂O₉) may also occur following the reaction:



2.1 CeGaO₃ stability.

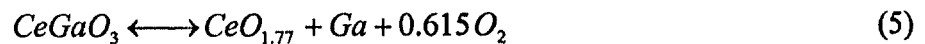
Leonov *et al.* [10] tried to synthesize CeGaO₃ from molar ratios of Ce₂O₃/Ga₂O₃ equal to 1:1, 3:5 and 1:11. The synthesis was conducted in oxidizing and inert gas environments at temperatures from 1273 K to 1973 K. No chemical compounds of defined structure or solid solutions were formed.

When the synthesis was conducted in H₂ or NH₃ at 1273 K, CeGaO₃ reportedly formed. However, completeness of the reaction was not achieved even in the case of repeated heating

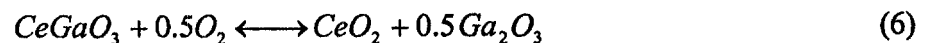
with intermediate grinding. Synthesis at 1573, 1673 and 1773 indicated that gallium oxide is intensively volatilized. Leonov *et al.* were able to synthesize CeGaO₃ in an evacuated and sealed quartz tube at 1573 K by the reaction:



The stability limits of the CeGaO₃ and PuGaO₃ compounds have been predicted by theoretical calculations performed by Stan *et al.* [1, 11, 12]. Examination of isothermal $\Delta G(O_2)$ change with composition for the Ce-O and Ga-O binaries suggest that CeGaO₃ undergoes a reducing disproportionation by the reaction



Based on the thermochemical representation of the CeO_{2-x} properties proposed by Lindemer [13], the partial pressure of oxygen resulted in $\log(P_{O_2}) = -12.77$. Solving the $\Delta G_{\text{reaction}}$ equation yields $\Delta G_f^{\text{CeGaO}_3}$ equal to -96.3 kJ/mole. Further examination of $\Delta G(O_2)$ change with composition suggest that CeGaO₃ undergoes an oxidizing disproportionation by the reaction



Using the previously calculated value for $\Delta G_f^{\text{CeGaO}_3}$, the $\log(P_{O_2})$ was calculated to be -4.91. Similar calculations have been performed at 500 K and 1000 K. The linear interpolation of the results leads to the following expression for the CeGaO₃ Gibbs free energy of perovskite phase formation:

$$\Delta G_f < CeGaO_3 > = -144.47 + 0.030641 T \text{ (kJ/mol)} \quad (7)$$

The partial pressure of oxygen was calculated for both the reducing reaction (5):

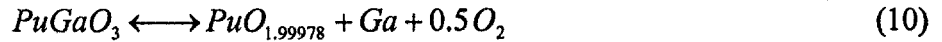
$$\log(PO_2) = 11.510 - \frac{38116.2}{T} \quad (8)$$

and the oxidation reaction (6):

$$\log(PO_2) = 7.824 - \frac{20241.5}{T} \quad (9)$$

2.2 PuGaO₃ Stability.

Similar calculations, based on the thermochemical representation of the PuO_{2-x} properties proposed by Besmann and Lindemer [14] and the examination of the reducing disproportionation reaction:



as well as the oxidizing disproportionation by the reaction:



resulted in the following expressions for the Gibbs free energy of PuGaO₃ perovskite phase formation:

$$\Delta G_f < PuGaO_3 > = -141.19 + 0.029725 T \text{ (kJ/mol)} \quad (12)$$

The partial pressure of oxygen was calculated for both the reducing reaction (10):

$$\log(PO_2) = 11.532 - \frac{38128.8}{T} \quad (13)$$

and the oxidation reaction (11):

$$\log(PO_2) = 5.856 - \frac{19106.5}{T} \quad (14)$$

Based on the dependency of the partial pressure of oxygen on temperature, at thermodynamic equilibrium, the limits of stability for the CeGaO₃ and PuGaO₃ perovskite phases can be calculated. The stability diagram (Fig. 2) shows how similar the limits are, further

supporting the use of cerium oxides as surrogates for the plutonium oxides, for thermodynamic modeling purposes.

One can note that, according to these calculations, the perovskite structures cannot be obtained in normal conditions of atmospheric oxygen pressure (in air). If the partial pressure of oxygen is 10^{-10} atm then both compounds are stable between almost the same limits (715 to 1250 K). For a partial pressure of oxygen of 10^{-20} atm, the stability limits are 1100-1825 K for CeGaO_3 and 1173-1825 K for PuGaO_3 . It was predicted that for generating the perovskite phase a reducing atmosphere is required.

3. EXPERIMENTAL

3.1 Sample preparation and thermal treatment

The samples were prepared using CeO_2 and Ga_2O_3 powders. Since the vaporization of the gallium oxides is expected at high temperatures, the initial compositions were calculated to provide Ga_2O_3 in excess in the system. Table 1 shows the initial compositions and the equivalent Ce_2O_3 - Ga_2O_3 molar content, calculated for the case when CeO_2 was completely reduced to Ce_2O_3 .

The densities of the green pellets, calculated by measuring volume and then weighting, were 7.65 g/cm^3 for CeO_2 , and 6.44 g/cm^3 for Ce_2O_3 . The theoretical densities were calculated on a mass percentage basis for the respective powders used.

The powders were prepared and milled for 20 minutes and then were pressed to 55-60 % of their theoretical densities and fired. A four-hour burnout starting at 523 K was followed by four hours of thermal treatment at 1273, 1473, and 1673 K in air, Ar, and Ar-6% H_2 environments (for

each temperature). The partial pressure of oxygen in the argon flow was determined to be lower than 100 ppm. Based on a model of the chemical reactions in the furnace [15], the logarithm of the partial pressure of oxygen in the Ar 6% H_2 mixture was -17.5 at 1273 K, -12.9 at 1473 K, and -9.5 at 1673 K.

The subsequent pellets were sectioned using a low speed saw. Half of the pellet was ground into a powder for x-ray analysis. The other half was polished and examined by SEM.

3.2 X-ray diffraction analysis (XRD).

The x-ray diffraction measurements were performed on a Scintag XDS 2000 with theta-theta geometry using $\text{CuK}\alpha_{1/2}$ radiation, and a graphite secondary monochromator. Phase identification was performed by using the Diffraction Management System software, version 1.3 (Scintag, Inc.). The peak identification was completed with MicroPower Diffraction Search Match software, version 4.30 (Fein-Marquart Associates, Inc.). Both software packages using the phase information provided by the ICDD PC-PDF 42 database. Rietveld crystal structure refinement were performed using the GSAS software package [16].

3.3 Scanning electron microscopy (SEM).

The microstructure of the samples was investigated by means of a JEOL 6300FVX field emission scanning electron microscope. The backscatter mode was preferred because allows for identification of phases based on the dependency of the contrast upon the average Z number.

4. RESULTS AND DISCUSSION

4.1 X-ray results

The results of the preliminary x-ray diffraction patterns analysis are shown in Table 2. As expected, the analysis of the samples fired in air (samples S1-S3) resulted in the two stable oxides CeO_2 and Ga_2O_3 . The same result was obtained for similar samples when the thermal treatment in air was followed by quenching. It should be noted that the samples are bluish colored, indicating the presence of nonstoichiometric CeO_{2-x} .

In the samples with C50 composition (S4-S6), thermally treated in argon atmosphere, the phases CeO_2 and Ga_2O_3 were identified. Few unmatched peaks with low intensities indicate the present of at least one additional phase, which could not be identified.

The samples fired under H_2/Ar conditions (S7-S9) show the formation of relatively large amounts of a new phase at temperatures of 1273 and 1473 K. This phase was identified to be CeGaO_3 with perovskite-type crystal structure. At 1673 K, CeO_2 and Ga_2O_3 are present with a few unindexed lines of a third phase.

The samples of C40, C60 and C80 composition (S10-S15) thermally treated in air or argon 6% H_2 , at 1673 K, show (besides the CeO_2 and Ga_2O_3 lines) some unindexed lines belonging to a third phase. In most cases, the intensity of the lines was small, preventing further refinement.

Advanced x-ray diffraction pattern analysis was performed on the samples where a third phase was present in significant amounts. The crystal structure of the expected CeGaO_3 was refined based on the structure description by Guitel *et al.* (1976) [7] of the isostructural rare earth gallate GdGaO_3 . Rietveld structure analyses were performed using the GSAS package [16]. No internal standard was added. Applying Least Square and Rietveld structure refinement and X-ray powder data, the orthorhombic space group (Pnma, 62) was confirmed for the CeGaO_3

perovskite structure. CeGaO_3 is also isostructural with the wide range of rare earth orthoferrites as described by Marezio *et al.* (1970) [17]. The Rietveld structure refinement of CeGaO_3 result in refinement residuals of $R_p = 9.2\%$ (Figure 3). R_p was defined as:

$$R_p = \frac{\sum |I_{obs} - I_{calc}|}{\sum I_{obs}}$$

The structure of CeGaO_3 is described in Table 3 in regard of lattice parameters and atomic positions.

4.2 SEM results

Fig. 4 shows a backscattering SEM image of the sample S8. One can note the separation of the two main phases Ga rich (dark area) and Ce rich (bright area). We have estimated that for the C50 composition samples, 43% of the area should be Ga rich and 57% should be Ce rich. The estimate was based on determining the volume V of each phase by dividing the preparation weights (Table 1) by the densities. Then area was approximated to be $A = V^{2/3}$. The ratio of the area occupied by the two phases, as appears in the SEM picture, is in good agreement with the estimation.

4.3 Discussion

For comparison, the calculated stability limits and the experimental results are illustrated in fig. 5. The perovskite phase formed in a significant amount (enough to be identified by X-ray analysis) for temperatures and oxygen partial pressures predicted by the thermodynamic calculations. Close to the calculated limits of stability, unindexed lines in the x-ray patterns suggest there was a third phase present, most likely the same perovskite compound. The phase did not form outside the calculated limits of the stability.

5. CONCLUSIONS

We have demonstrated that the CeGaO_3 perovskite phase, previously predicted by the theoretical thermodynamic calculations, can in fact be produced under conditions relevant to the processing and operation of MOX fuel, in the CeO_2 - Ga_2O_3 system.

Based on the available thermodynamic data for the binary subsystems of the Ce-Ga-O and the Pu-Ga-O systems, we have estimated the stability limits of the CeGaO_3 and PuGaO_3 compounds. Mixtures of CeO_2 and Ga_2O_3 have been prepared taking into account the possible reduction of CeO_2 to Ce_2O_3 at high temperatures. To confirm the predicted influence of the partial pressure of oxygen, separate sets of samples of the same composition have been treated in atmosphere of air, argon or Ar 6% H_2 , at temperatures between 1273 and 1473 K.

A preliminary x-ray diffraction pattern analysis revealed the occurrence of new phase. Based on Rietveld structure refinement of X-ray powder data, the CeGaO_3 perovskite structure was identified as belonging to the orthorhombic space group (Pnma, 62). The lattice parameters are: $a = 5.484(1)$, $b = 7.747(1)$, and $c = 5.490(1)$ Å.

Analyzing the conditions in which the compound was obtained, it becomes credible that the reducing atmosphere improves the chances of formation of the perovskite phase, while the neutral (Argon) atmosphere diminishes these chances. It seems to be rather unlikely to form crystalline perovskite-type CeGaO_3 in air.

We may reasonably extrapolate that the PuGaO_3 compound may be present at low concentrations in the weapons grade PuO_2 powder. Since this compound is a solid at the temperatures where Ga removal or pellet sintering is conducted, it therefore may control the limit for Ga removal.

REFERENCES

- [1] H. R. Trellue, T. Baros, H.T. Blair, J. J. Buksa, D. P. Butt, K. Chidester, S. F. DeMuth, S. L. Eaton, G. L. Havrilla, R. J. Hanrahan, Jr., C. A. James, D. G. Kolman, R. E. Mason, Y. Park, M. Stan, J. H. Steele, Jr., S. S. Vos, T. C. Wallace, Sr., C. G. Worley, "Nuclear Fuels Technologies Fiscal Year 1997 Research and Development Test Results", Los Alamos National Laboratory Report, LA-UR-97-4423, 1997.
- [2] J. R. Schoonover, A. Saab, J. S. Bridgewater, G. J. Havrilla, C. T. Zugates, and P. J. Treado, "Raman/SEM Chemical Imaging of a Residual Gallium Phase in a Mixed Oxide Feed Surrogate", *App. Spectrosc.*, **54**, 1362-1371 (2000).
- [3] R. J. Hanrahan Jr, Billy W. Roybal, Michele B. Gross, and Stacey L. Eaton, "UO₂ - CeO₂ - Ga₂O₃ Sintering Studies: Effects of Gallia on the Sintering Kinetics of Ammonium-Uranyl Carbonate (AUC) Process Uranium Dioxide", Los Alamos National Laboratory Report, LA-UR-99-2742, 1999.
- [4] D. Grier, and G. McCarty, North Dakota State University, Fargo, North Dakota, ICDD Grant-in Aid, 1991.
- [5] M. Marezio, J. P. Remeika, and P. D. Dernier, "Rare Earth Orthogallates", *Inorg. Chem.*, **7**, 1337-1340 (1968).
- [6] S. Geller, P.J. Curlander, and G.F. Ruse, "Perovskite-Like Rare Earth Gallium Oxides Prepared at Atmospheric Pressure", *Mat. Res. Bull.* **9**, 637-644 (1979).

- [7] J.C. Guitel, M. Marezio, J. Mareschal, "Single-Crystal Synthesis and Structural Refinement of GdGaO_3 ", *Mater. Res. Bull.*, **11**, 739-744 (1976).
- [8] T. Shishido, Y. Zheng, A. Saito, H. Horiuchi, K. Kudou, S. Okada, and T. Fukuda, "Microstructure, Thermal Properties and Hardness of the CeMo_3 ($\text{M} = \text{Al, Ga}$) Synthesized by Arc-Melting Method", *J. Alloys Comp.* **260**, 88-92, (1997).
- [9] Y. Kanke and A. Navrotsky, "A calorimetric Study of the Lanthanide Aluminum Oxides and the Lanthanide Gallium Oxides: Stability of the Perovskites and the Garnets", *J. Solid State Chem.*, **141**, 424-436 (1998).
- [10] A. I. Leonov, A. V. Andreeva, V. E. Shvaiko-Svaikovskii, and E. K. Keler, "High Temperature Chemistry of the Cerium in the Systems Cerium Oxides- Al_2O_3 , Cr_2O_3 , Ga_2O_3 ", *Izvestiya Akademii Nauk SSSR, Neorganicheskie Materialy*, **2**, 517-523 (1966).
- [11] D. P. Butt, R. J. Hanrahan, Jr., Y. Park, M. Stan, and T. C. Wallace, Sr., "Thermodynamics and Kinetics of Ga in MOX", Los Alamos National Laboratory Report, LA-UR-97-3853, 1997.
- [12] D. P. Butt, R. J. Hanrahan, Jr., Y. Park, and M. Stan, "Thermodynamics, Phase Relationships, and the Kinetics of Gallium Removal from Mixed Oxide Fuel Fabricated with Weapons Grade Plutonium", Los Alamos National Laboratory Report, LA-UR-97-4719, 1997.
- [13] T. B. Lindemer, "Chemical Thermodynamic Representation of Very Nonstoichiometric Phases: $\langle \text{CeO}_{2-x} \rangle$ ", *CALPHAD* **10**, 129-136 (1986).
- [14] T. M. Besmann and T. B. Lindemer, "Chemical Thermodynamic Representation of $\langle \text{PuO}_{2-x} \rangle$ and $\langle \text{U}_{1-z}\text{Pu}_z\text{O}_w \rangle$ ", *J. Nucl. Mat.*, **130**, 489-504 (1985).

- [15] D.G. Kolman, T.N. Taylor, Y.S. Park, M. Stan, D.P. Butt, C.J. Maggiore, J.R. Tesmer, and G.J. Havrilla, "Gallium-Suboxide Attack of Stainless Steel and Nickel Alloys at 800-1200 degrees C", *Oxidation of Metals*, **55**, 439-472 (2001).
- [16] A.C. Larson and R.B. Von Dreele, "General Structure Analysis System", Los Alamos National Laboratory Reports, LA-UR-86-748, 1986.
- [17] M. Marezio, J.P. Remeika, P.D. Dernier, "The Crystal Chemistry of the Rare Earth Orthoferrites", *Acta Cryst.*, **B26**, 2008-2022 (1970).

FIGURE CAPTIONS

Fig. 1. Gibbs free energy of formation of several oxides.

Fig. 2. Calculated limits of stability for the CeGaO_3 and PuGaO_3 compounds.

Fig. 3. Rietveld structure refinement of orthorhombic CeGaO_3 perovskite.

Fig. 4. Backscattered SEM image of the sample S10 (perovskite composition, fired in Ar at 1673 K). Light areas are Ce rich, dark areas are Ga rich.

Fig. 5. Calculated stability limits and experimental results for the CeGaO_3 perovskite compound.

Table 1. The initial composition of the samples

Comp. Label	Theoretical sesquioxide content (mole fractions)		Actual initial composition			
			(mole fractions)		(grams)	
	Ga_2O_3	Ce_2O_3	Ga_2O_3	CeO_2	Ga_2O_3	CeO_2
C40	0.4	0.6	0.250	0.750	2.663	7.337
C50	0.5	0.5	0.333	0.667	3.526	6.474
C60	0.6	0.4	0.429	0.571	4.496	5.504
C80	0.8	0.2	0.667	0.333	6.854	3.146

Table 2. Comparison of the experimental data and calculated X-ray patterns

Sample	Comp	Thermal treatment	Atmosphere	Matched phases	Unmatched d-spacing (Å) and intensity (in parentheses)
S1	C50	1000	Air	CeO ₂ , Ga ₂ O ₃	
S2	C50	1200	Air	CeO ₂ , Ga ₂ O ₃	
S3	C50	1400	Air	CeO ₂ , Ga ₂ O ₃	
S4	C50	1000	Ar	CeO ₂ , Ga ₂ O ₃	2.7366 (6), 1.6266 (22)
S5	C50	1200	Ar	CeO ₂ , Ga ₂ O ₃	2.7426 (4.4)
S6	C50	1400	Ar	CeO ₂ , Ga ₂ O ₃	2.7404 (6.7), 2.7331 (4.8)
S7	C50	1000	Ar/H ₂	CeO ₂	3.8640 (11), 3.4610 (2.5), 2.7348 (100), 2.2326 (11), 1.9353 (25), 1.9058 (1.9), 1.8824 (1.9), 1.8758 (1.7), 1.7303 (4.2), 1.6886 (2.5), 1.5813 (32), 1.3692(12), 1.3671 (8.1)
S8	C50	1200	Ar/H ₂	none	3.8744 (8.16), 3.1154 (4.98), 3.0493 (3.51), 2.7391 (100), 2.2390 (11.56), 1.9371 (22.98), 1.7348 (3.32), 1.6921 (2.49), 1.5826 (32.51), 1.3707 (37.07), 2.7404 (6.7), 2.7331 (4.8)
S9	C50	1400	Ar/H ₂	CeO ₂ , Ga ₂ O ₃	3.081 (4.2), 2.7331 (2.9), 1.5609 (9.5)
S10	C40	1400	Ar	CeO ₂ , Ga ₂ O ₃	
S11	C40	1400	Ar/H ₂	CeO ₂	3.875 (5), 3.074 (5.4), 3.034(5.0), 2.7384 (51), 1.9380 (15), 1.5817 (13), 1.5804 (13), 1.3708 (7.8), 1.3671 (4.1)
S12	C60	1400	Ar	CeO ₂ , Ga ₂ O ₃	2.7306 (4.4), 1.5382 (2.1)
S13	C60	1400	Ar/H ₂	CeO ₂ , Ga ₂ O ₃	2.9529 (1.8), 2.5773 (3.3), 1.6386 (4.2), 1.6219 (5.4)
S14	C80	1400	Ar	CeO ₂ , Ga ₂ O ₃	
S15	C80	1400	Ar/H ₂	CeO ₂ , Ga ₂ O ₃	2.7366 (9.5), 1.9738 (7.5), 1.5279 (5.2), 1.5197 (9.2)

Table 3: The crystal structure of CeGaO₃ Cerium Gallate

CeGaO ₃	Cerium Gallate		Space Group <i>P n m a</i> (62)	
Lattice Parameter [Å]	<i>a</i> = 5.484(1)	<i>b</i> = 7.747(1)	<i>c</i> = 5.490(1)	<i>Z</i> = 4
Atomic Positions	Wyckoff Letter	<i>x</i> (standard deviation)	<i>y</i> (standard deviation)	<i>z</i> (standard deviation)
Ce	4 c	0.02759 (0.0002)	0.25	0.9954 (0.0004)
Ga	4 b	0.50	0.00	0.00
O-1	4 c	0.4895 (0.0017)	0.25	0.0889 (0.0022)
O-2	8 d	0.2807 (0.0026)	0.0318 (0.0014)	0.7277 (0.0030)

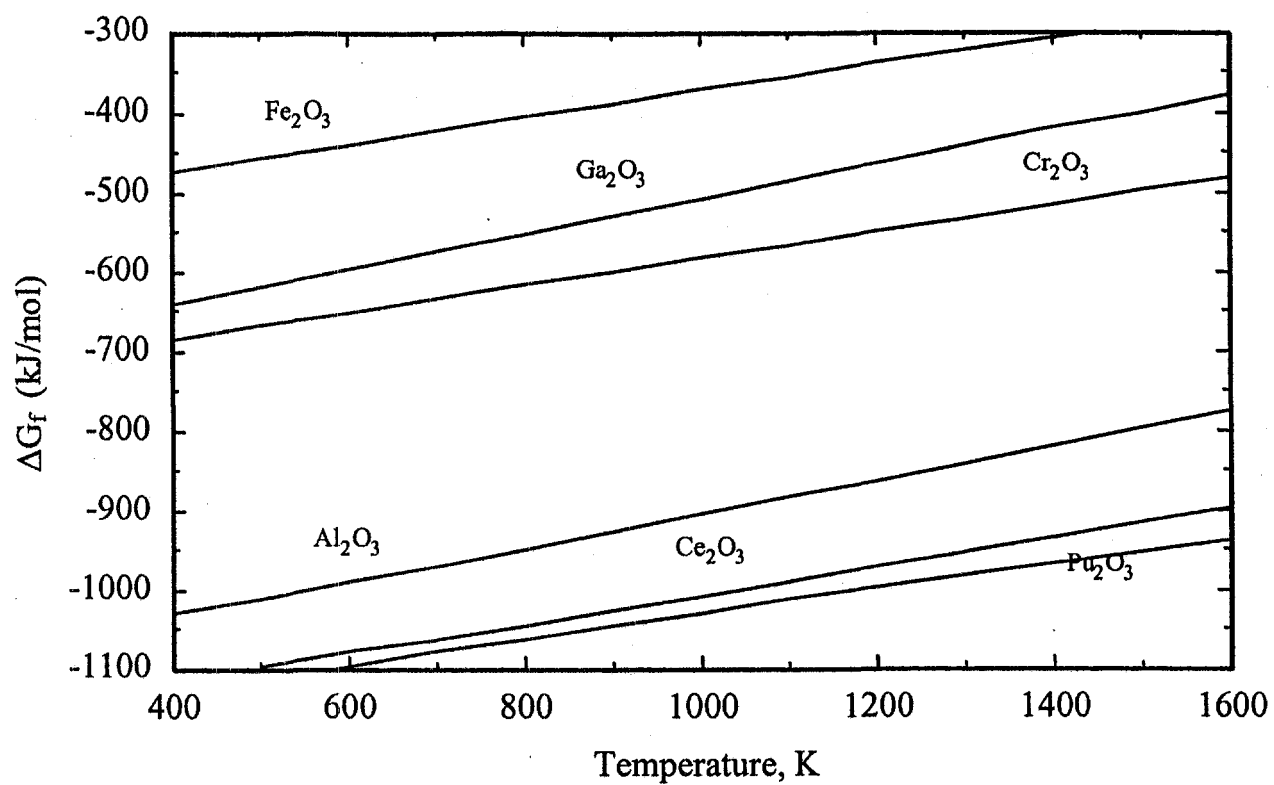


Fig. 1. Gibbs free energy of formation of several oxides.

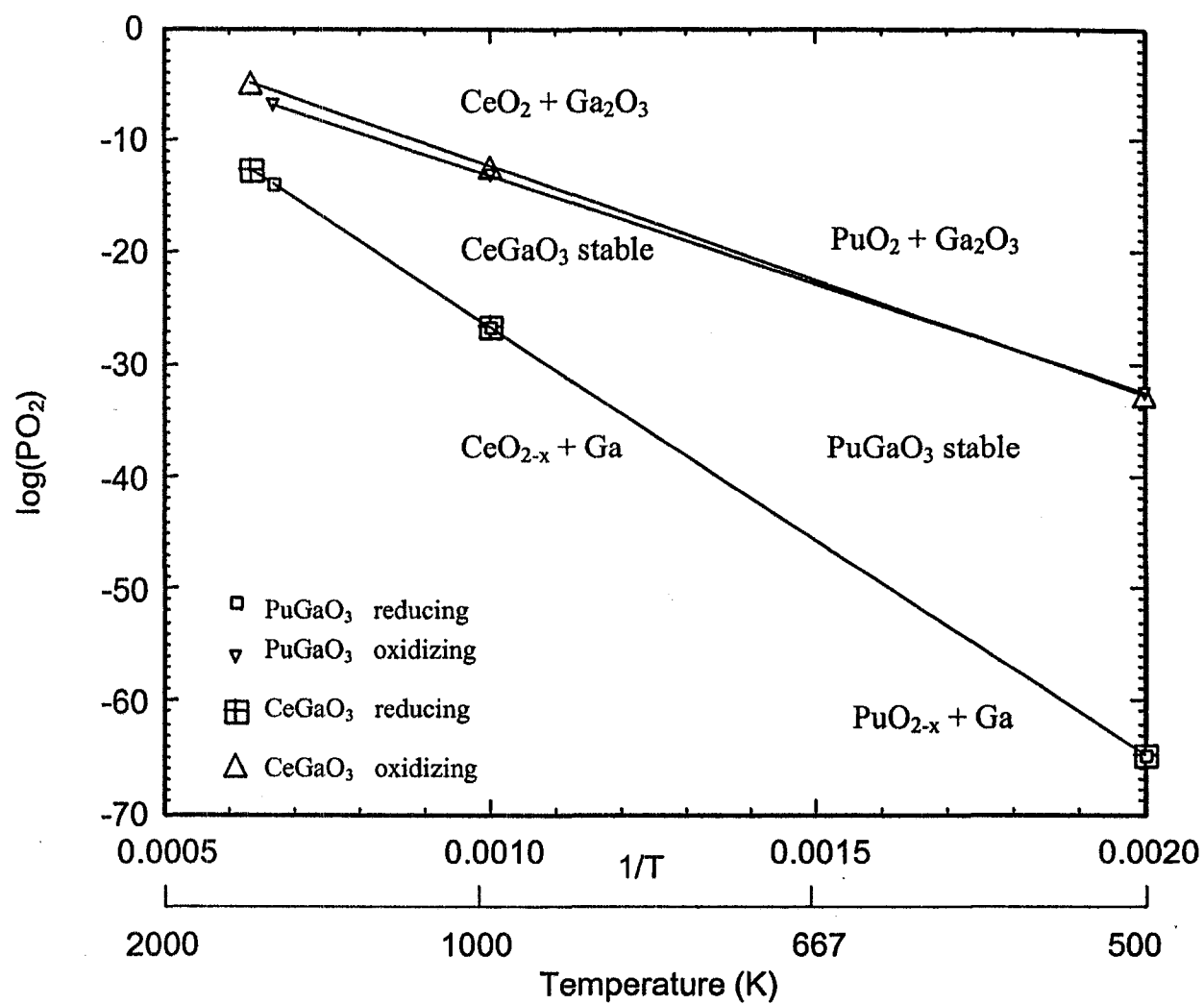


Fig. 2. Calculated limits of stability for the CeGaO_3 and PuGaO_3 compounds.

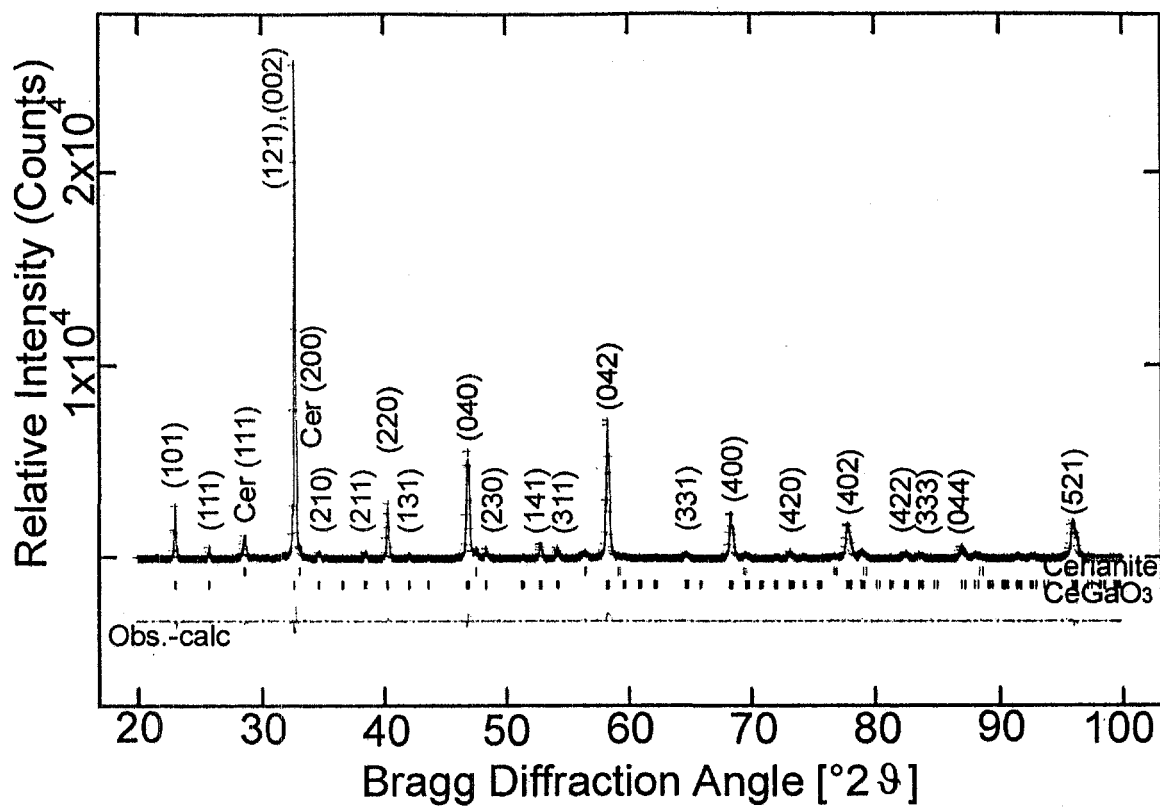


Fig. 3. Rietveld structure refinement of orthorhombic CeGaO_3 perovskite.

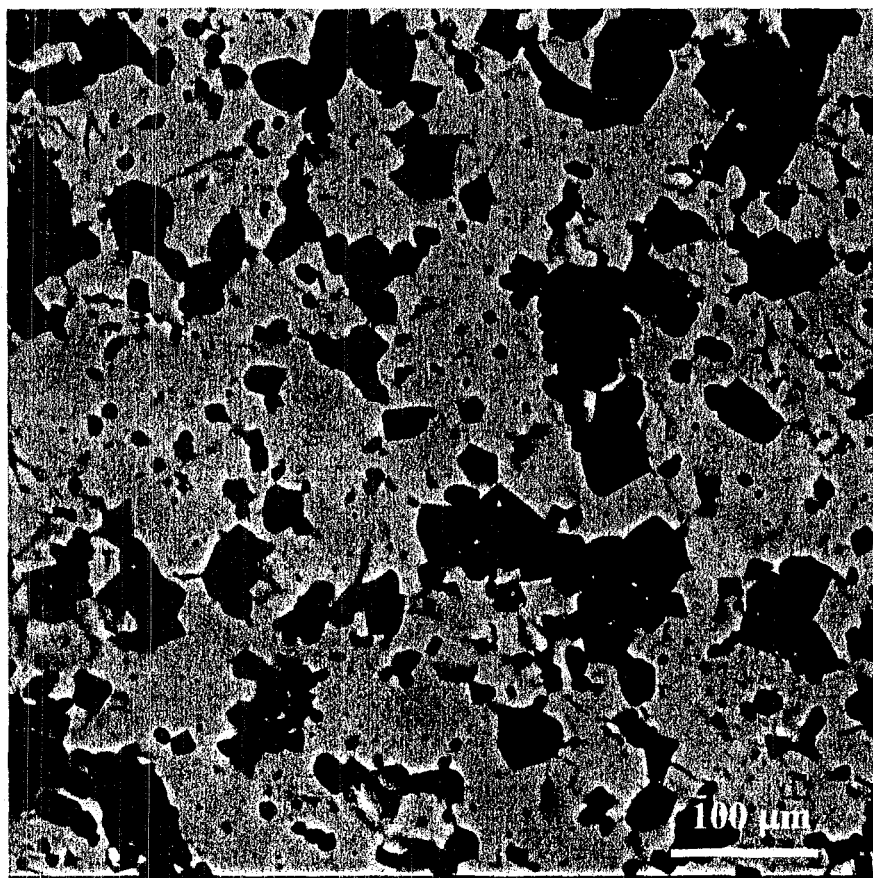


Fig. 4. Backscattered SEM image of the sample S10 (perovskite composition, fired in Ar at 1673 K). Light areas are Ce rich, dark areas are Ga rich.

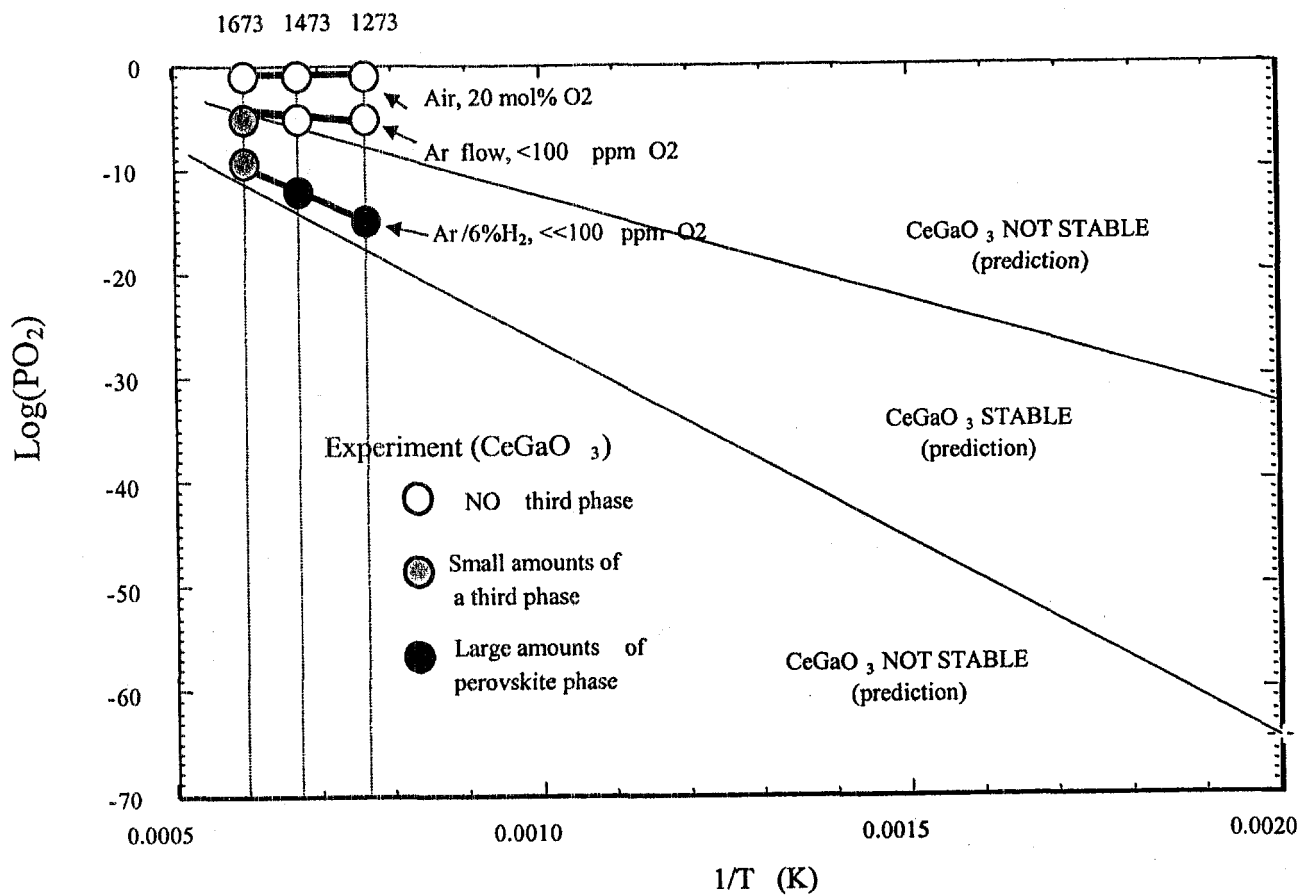


Fig. 5. Calculated stability limits and experimental results for the CeGaO₃ perovskite compound.